THE JOURNAL OF BIOLOGICAL CHEMISTRY
Vol. 275, No. 47, Issue of November 24, pp. 36794–36802, 2000

Printed in U.S.A.

Carboxyl-terminal Fragments of Alzheimer β-Amyloid Precursor Protein Accumulate in Restricted and Unpredicted Intracellular Compartments in Presenilin 1-deficient Cells*

Received for publication, August 2, 2000, and in revised form, August 23, 2000
Published, JBC Papers in Press, August 28, 2000, DOI 10.1074/jbc.M006986200

Fusheng Chen‡, Dun-Sheng Yang‡, Suzana Petanceska§, Austin Yang§, Anurag Tandon‡, Gang Yu‡, Richard Rozmahel¶, Jorge Ghiso§, Masaki Nishimura‡, Dong Mei Zhang‡, Toshitaka Kawarai‡, Georges Levesque‡, Julia Mills‡, Lyne Levesque‡, You-Qiang Song‡, Ekaterina Rogaeva‡, David Westaway‡, Howard Mount‡, Sam Gandy§, Peter St George-Hyslop‡‖, and Paul E. Fraser‡

From the ‡Centre for Research in Neurodegenerative Diseases, Departments of Laboratory Medicine and Pathobiology, Medical Biophysics and Medicine, University of Toronto, and Department of Medicine (Neurology), Toronto Hospital, Toronto, Ontario M5S 3H2, Canada, the §Departments of Psychiatry and Pathology, New York University School of Medicine, Nathan S. Kline Institute, Orangeburg, New York 10962-2210, the ¶Departments of Pharmacology and Genetics, Research Institute, Hospital for Sick Children, Department of Genetics, Toronto, Ontario M5S 3H2, Canada and the Department of Pharmacology, University of Toronto, Toronto, Ontario M5S 3H2, Canada

Absence of functional presenilin 1 (PS1) protein leads to loss of γ-secretase cleavage of the amyloid precursor protein (βAPP), resulting in a dramatic reduction in amyloid β peptide (Aβ) production and accumulation of α- or β-secretase-cleaved COOH-terminal fragments of βAPP (α- or β-CTFs). The major COOH-terminal fragment (CTF) in brain was identified as βAPP-CTF-(11–98), which is consistent with the observation that cultured neurons generate primarily Aβ-(11–40). In $PS1^{-/-}$ murine neurons and fibroblasts expressing the loss-of-function $PS1_{D385A}$ mutant, CTFs accumulated in the endoplasmic reticulum, Golgi, and lysosomes, but not late endosomes. There were some subtle differences in the subcellular distribution of CTFs in $PS1^{-/-}$ neurons as compared with $PS1_{D385A}$ mutant fibroblasts. However, there was no obvious redistribution of full-length βAPP or of markers of other organelles in either mutant. Blockade of endoplasmic reticulum-to-Golgi trafficking indicated that in $PS1^{-/-}$ neurons (as in normal cells) trafficking of βAPP to the Golgi compartment is necessary before α- and β-secretase cleavages occur. Thus, although we cannot exclude a specific role for PS1 in trafficking of CTFs, these data argue against a major role in general protein trafficking. These results are more compatible with a role for PS1 either as the actual γ-secretase catalytic activity or in other functions indirectly related to γ-secretase catalysis (*e.g.* an activator of γ-secretase, a substrate adaptor for γ-secretase, or delivery of γ-secretase to βAPP-containing compartments).

* This work was supported by grants from the Medical Research Council of Canada, Alzheimer Association of Ontario, Howard Hughes Medical Research Foundation, Scottish Rite Charitable Foundation, Helen B. Hunter Fellowship (to G. Y.), and the Peterborough Burgess Fellowship (to E. R.); by a University of Toronto Department of Medicine postgraduate fellowship (to M. N.); and by the Japan Society for the Promotion of Science (to T. K.), the United States Public Health Service (S. G.), and the Research Foundation for Mental Hygiene of the New York State Office of Mental Health (to S. G.). The costs of publication of this article were defrayed in part by the payment of page charges. This article must therefore be hereby marked "*advertisement*" in accordance with 18 U.S.C. Section 1734 solely to indicate this fact.

‖ To whom correspondence could be addressed: Centre for Research in Neurodegenerative Diseases, University of Toronto, 6 Queen's Park Crescent W., Toronto, Ontario M5S 3H2, Canada. Fax: 416-978-1878; E-mail: p.hyslop@utoronto.ca.

The presenilin 1 (PS1)[1] and presenilin 2 (PS2) genes encode polytopic transmembrane proteins (1, 2), which are components of high molecular weight, multimeric protein complexes predominantly located in the nuclear envelope, endoplasmic reticulum (ER), Golgi, and selected intracellular vesicular structures (3–9). These proteins play major roles in controlling the proteolytic processing of *Notch* and the β-amyloid precursor protein (βAPP) (10–15). Absence of PS1 is associated with failure of γ-secretase-mediated cleavage of the COOH-terminal fragments (CTFs) generated by α- or β-secretase cleavage of the βAPP (10–12). Thus, PS1 deficiency results in accumulation of the CTFs of βAPP and a dramatic reduction in Aβ production.

The mechanism by which absence of PS1 function causes loss of γ-secretase activity is unclear; but the observations that 1) mutation of two transmembrane aspartate residues in PS1 (Asp^{257} and Asp^{385}) causes loss of γ-secretase cleavage; and 2) transition state aspartyl protease inhibitors, which block γ-secretase activity bind to PS1 and PS2 (16, 17), have led to speculation that PS1 may itself be a novel aspartyl protease with γ-secretase activity (18). However, we have recently observed that aspartyl mutants disrupt the maturation of PS1 into high molecular weight functional complexes (19). Consequently, alternate explanations for the roles of PS1 in the processing of type 1 transmembrane proteins like βAPP and *Notch* must be formally evaluated (11, 13). For instance, PS1 might be involved in the trafficking of selected substrate proteins to site(s) where γ-secretase cleavage occurs (11). It is also possible that PS1 serves as an adaptor for the βAPP/γ-secretase reaction or that it is necessary for the activation or trafficking of γ-secretase itself. To address these questions, we have investigated the intracellular distribution of COOH-terminal βAPP derivatives in homogenates from $PS1^{-/-}$ mouse

[1] The abbreviations used are: PS1, presenilin 1; PS2, presenilin 2; βAPP, β-amyloid precursor protein; CTF, COOH-terminal fragments of β-amyloid precursor protein arising from α-secretase or β-secretase cleavage; ER, endoplasmic reticulum; SELDI, surface-enhanced laser desorption/ionization; Aβ, amyloid β-peptide; NTF, NH_2-terminal fragments of β-amyloid precursor protein; BFA, brefeldin A; TGN, *trans*-Golgi network; sER, smooth endoplasmic reticulum; FL-βAPP, full-length β-amyloid precursor protein; NCZ, nocodazole; PNS, postnuclear supernatant; PBS, phosphate-buffered saline; MES, 4-morpholineethanesulfonic acid; Tricine, *N*-tris(hydroxymethyl)methylglycine.

brain, in cultured PS1$^{-/-}$ mouse neurons, and in murine fibroblasts expressing the PS1$_{D385A}$ loss-of-function mutation, paying particular attention to those intracellular compartments (ER, Golgi, endosome-lysosome endocytic pathway, and caveolae) previously associated with Aβ peptide generation. We have also investigated the early trafficking events that precede the accumulation of βAPP CTFs in these same tissues. Our data indicate that, in the absence of functional PS1, CTFs accumulate in a subset of the putative intracellular sites of Aβ generation (*i.e.* ER and Golgi, but not late endosomes). These experiments also indicate that trafficking of full-length βAPP (FL-βAPP) at least as far as the Golgi apparatus is required before βAPP-CTFs begin to accumulate. Presenilin deficiency causes no obvious abnormality in the subcellular distribution of FL-βAPP or organelle marker proteins.

MATERIALS AND METHODS

PS1 Null Mice—Mice lacking functional expression of PS1 were generated using homologous recombination to introduce a neomycin cassette flanked by *loxP* sequences approximately 200 base pairs downstream of exon 5 of the murine PS1 gene. When the *loxP* flanked neomycin cassette is not removed by *cre* recombinase, the presence of cryptic splice sites within the neomycin cassette results in the generation of extremely low quantities of unstable transcripts which lack an open reading frame after exon 5.[2] These transcripts result in no detectable PS1 protein expression in ES cells or in the brains of animals homozygous for this construct. As expected, homozygous PS1-deficient mice (PS1$^{-/-}$) displayed the previously reported skeletal abnormalities as well as absent γ-secretase activity (20, 21).

PS1$_{D385A}$ Cells—Wild type murine fibroblasts were transformed with human PS1$_{D385A}$ mutant cDNA using the pREV retroviral vector (CLONTECH). Functional expression was confirmed using species-specific antibodies to show replacement of endogenous murine PS1 by the mutant human PS1 (22).

Electron Microscopy—Brain tissue was obtained from 2-month-old PS1$^{-/-}$ or PS1$^{+/+}$ mice and was prepared for electron microscopy as described previously (23). Brain pieces were fixed with 4% paraformaldehyde, 0.2% glutaraldehyde. Vibratome sections (70–100 μm) were cut and processed with the ABC method, using the anti-βAPP COOH-terminal antibody 369. The sections were post-fixed in 2% glutaraldehyde overnight and in 1% osmium tetroxide for 1 h. The sections were then dehydrated, flat embedded in Epon, and polymerized. Ultrathin sections were cut, stained with uranyl acetate and lead citrate, and viewed with a Hitachi H-7000 electron microscope.

Electron microscopic ultrastructural analysis of the biochemical membrane fractions confirmed their authenticity as described (Fig. 1) (24, 25). The fractions were fixed in glutaraldehyde (2% final concentration) and centrifuged at 100,000 × *g* for 30 min. The pellets were washed, post-fixed with 1% osmium tetroxide for 1 h, stained with 2% aqueous uranyl acetate, dehydrated, and embedded in Epon. Ultrathin sections were cut, stained with lead citrate, and examined by electron microscopy.

Subcellular Fractionation—Two methods were used to isolate ER and Golgi-enriched fractions from mouse brain tissue. Brains were homogenized in 2 ml of 0.25 M sucrose in buffer A (5 mM HEPES, 1 mM EDTA, pH 7.2, and 5 μg/ml chymostatin, pepstatin, leupeptin, and antipain), and centrifuged at 1,000 × *g* for 10 min. The postnuclear supernatant (PNS) was then layered on a discontinuous sucrose gradient containing four step concentrations of sucrose in buffer A (1 ml/2.0 M, 3.4 ml/1.3 M, 3.4 ml/1.0 M, and 2.7 ml/0.6 M), and centrifuged at 280,000 × *g* for 2 h at 4 °C (26, 27). Twenty-four 0.5-ml fractions were collected from the bottom of the centrifugation tube. ER and Golgi membranes were also separated in independent experiments using iodixanol gradients (28). Brain tissue was homogenized in 1.5 ml of buffer (130 mM KCl, 25 mM NaCl, 25 mM Tris, 1 mM EGTA, pH 7.4), and spun for 10 min at 1,000 × *g*. Supernatants were removed, spun for 10 min at 3,000 × *g*; layered on a step gradient consisting of 1 ml each of 30%, 25%, 20%, 15%, 12.5%, 10%, 7.5%, 5%, and 2.5% (v/v) iodixanol (Accurate) in homogenization buffer, and centrifuged at 126,000 × *g* for 30 min. Ten fractions were collected from the top of the gradient.

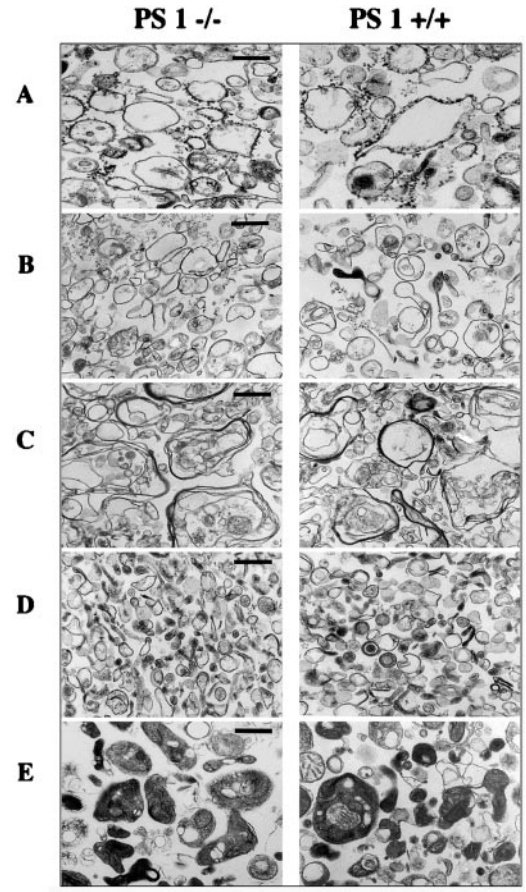

FIG. 1. **Electron micrographs of subcellular fractions prepared biochemically from brains of PS1$^{-/-}$ (*left panels*) or PS1$^{+/+}$ (*right panels*) mice showing the morphology of components from the rough endoplasmic reticulum (*A*), smooth endoplasmic reticulum (*B*), Golgi apparatus (*C*), late endosome (*D*), and lysosome (*E*) fractions.** *Scale bars*, 400 nm in *A*, *B*, and *D*; 600 nm in *C* and *E*.

Early and late endosome fractions were separated on a flotation gradient (29). After homogenization in 0.25 M sucrose in buffer A, the PNS was brought to 40.6% sucrose (final volume, 2.0 ml) and loaded at the bottom of a gradient consisting of 4 ml of 16% sucrose in buffer B containing 3 mM imidazole in D_2O (pH 7.4), 3 ml of 10% sucrose in buffer B, and 1 ml of homogenization buffer. The gradient was centrifuged at 160,000 × *g* for 1 h at 4 °C. The early and late endosomal fractions were collected at the 16%/10% sucrose interface and the uppermost portion of the 10% sucrose cushion, respectively.

Lysosomes and mitochondria were fractionated by two sequential density gradients (30). Initially, the PNS was loaded on a hybrid Percoll/metrizamide gradient, and centrifuged at 50,000 × *g* for 15 min. Mitochondria were collected from the 17%/35% metrizamide interface. The 6% Percoll/17% metrizamide interface was removed, adjusted to 35%, and placed at the bottom of the second gradient. After further centrifugation at 50,500 × *g* for 15 min, the lysosomes were collected from the 5%/17% metrizamide interface.

Caveolae-like membrane microdomains were purified by three methods (31–35). For detergent-free purification, the tissues were washed twice with ice-cold phosphate buffered saline (PBS) and homogenized in 2 ml of 500 mM sodium carbonate, pH 11.0. The homogenate was adjusted to 45% sucrose by the addition of 2 ml of 90% sucrose prepared in buffer C (25 mM MES, pH 6.5, 150 mM NaCl) and placed at the bottom of a 5–35% discontinuous sucrose gradient (4 ml of 5% sucrose, 4 ml of 35% sucrose; both in buffer C containing 250 mM sodium carbonate) and centrifuged at 275,000 × *g* for 18 h at 4 °C. Twelve 1-ml fractions were collected from the top of the gradient. The pellet from each fraction was diluted 10-fold in buffer C containing 1% sodium dodecyl sulfate (SDS) and an equal volume of Laemmli sample buffer. For detergent purification, the tissues were washed twice with ice-cold PBS and homoge-

[2] R. Rozmahel, F. Chen, D.-S. Yang, S. Petanceska, A. Yang, A. Tandon, G. Yu, J. Ghiso, M. Nishimura, D. M. Zhang, T. Kawarai, G. Levesque, J. Mills, L. Levesque, Y.-Q. Song, E. Rogaeva, D. Westaway, H. Mount, S. Gandy, P. St George-Hyslop, and P. E. Fraser, manuscript in preparation.

nized in 2 ml of buffer C with 1% Triton X-100 and 5 μg/ml chymostatin, pepstatin, leupeptin, and antipain. The homogenate was adjusted to 40% sucrose by addition of 2 ml of 80% sucrose in buffer C, placed under 8 ml of a linear 5–30% sucrose gradient in buffer C containing protease inhibitors as above, but lacking Triton X-100. The gradients were centrifuged, fractions were collected, and an aliquot of each fraction was used for immunoblotting. Caveolae were also purified by the immunoisolation method previously described (35) except that anti-flotillin antibodies were used instead of anti-caveolin antibodies. In agreement with some previous reports (31, 32, 34), both PS1 and βAPP were detectable in neuronal caveolae, which are biochemically defined by the presence of flotillin (33). However, βAPP-CTFs were inconsistently present in flotillin fractions when prepared by different methods, thus precluding any reliable conclusions (data not shown). These experiments were therefore not pursued further.

Electrophoresis and Immunoblotting—The proteins in each fraction were precipitated, dissolved in SDS sample buffer, and separated on 10–20% Tris-Tricine polyacrylamide gradient gels (Novex) for βAPP-CTF and FL-βAPP, and on Tris-glycine gels for PS1-NTF, PS1-CTF, and marker proteins. After transfer to polyvinylidene difluoride membrane (pore size, 0.1 μm; Millipore), Western blots were probed with antibodies to βAPP-CTF and FL-βAPP (antibody 369), PS1-NTF (antibody 14), and PS1-CTF (polyclonal antibody 1143). Marker proteins for specific organelles were detected by ECL (Amersham Pharmacia Biotech) with the appropriate antibodies for the ER (calnexin, Stressgene), Golgi (Rab6, Santa Cruz Biotechnology; β-COP, Sigma), *trans*-Golgi network (TGN)-to-plasma membrane transport vesicles (Rab8, Transduction Laboratories), lysosomes (cathepsin D, Biodesign), endosomes (Rab9 and Rab7, gift from Dr. S. Pfeffer), and caveolae (flotillin, Transduction Laboratories) (26, 27, 29).

Metabolic Labeling and Immunoprecipitation—Primary cultures of cerebellar granule neurons were obtained from dissociated cerebella of 6-day-old mice. Cells were plated in minimal essential medium (with 10% fetal bovine serum, 0.5% glucose, and 25 mM KCl) on poly-D-lysine-coated plastic 60-mm^2 dishes. 4 μM cytosine arabinoside was added 18 h after plating. Cultures were ~95% neuronal, as indicated by immunostaining with neuron-specific enolase.

After 7–9 days in culture, neurons were pre-incubated for 1 h in methionine-free and cysteine-free Dulbecco's modified Eagle's medium containing 25 mM KCl with or without brefeldin A (BFA; 2 μg/ml, Sigma) or nocodazole (NCZ; 10 or 30 μg/ml, Sigma). 100 μCi/ml Tran^{35}S-labeling reagent (ICN) was added for 2 h, and then the media were replaced with unlabeled conditioned medium for 4 h at 37 °C. In temperature block experiments, cells were pre-incubated in methionine- and cysteine-free medium at 16 °C for 45 min before the addition of Tran^{35}S-labeling reagent. Metabolic labeling continued at the respective temperature for 2 h, followed by a chase for 4 h in conditioned minimal essential medium at 16 °C or 37 °C. Cells were washed in cold PBS and then lysed in 1 ml of buffer (50 mM Tris, pH 7.5, 150 mM NaCl, 2 mM EDTA, 1% Nonidet P-40, and protease inhibitors) on ice for 30 min. The lysates were spun at 13,000 rpm for 5 min, and the FL-βAPP and α- and β-CTFs were immunoprecipitated with the polyclonal antibody 369 and analyzed by 10–20% Tris-Tricine SDS-polyacrylamide gel electrophoresis (Novex). Gels were dried and exposed to Kodak Biomax film, and the intensities of autoradiographic bands were measured by densitometry, corrected for the moles of methionine and cysteine residues per mole of FL-βAPP or βAPP-CTFs, and the data were expressed as a percentage of the initially labeled FL-βAPP at $t = 0$.

For secreted βAPP and Aβ immunoprecipitations, culture media were collected and immunoprecipitated using monoclonal antibodies 5A3/1G7 and polyclonal FCA18 as described (11, 36).

Immunoprecipitation of APP CTFs for Mass Spectrometry—Brains were removed from young PS1$^{-/-}$ mice or from non-transgenic Swiss Webster mice. Each brain was homogenized in 2% SDS/PBS buffer containing a mixture of protease inhibitors (Complete; Roche Molecular Biochemicals), at 1:10 w/v ratio. The homogenates were centrifuged at 100,000 × *g* for 30 min at room temperature. The supernatants were diluted 5-fold with 2.5% Triton X-100/PBS (to a final SDS concentration of 0.4%), and precleared by an overnight incubation with protein A-Sepharose beads. After removal of the protein A-Sepharose, ~5 mg of brain protein was immunoprecipitated using antiserum 369. The immunoprecipitated material was collected on protein A-Sepharose beads. The protein A-Sepharose beads were washed four times with 0.1%Triton X-100/PBS buffer, once in PBS and once in nanopure water.

Analyses of APP COOH-terminal Fragments by SELDI—Immunoprecipitated βAPP-CTFs on protein A beads were suspended in a microcentrifuge tube and washed three times with 1 ml of PBS containing 0.1% Triton X-100 (v/v) for 10 min and twice with 1 ml of HPLC-grade water. The sample was then air-dried for 15 min and mixed with 200 μl of α-cyano-4-hydroxycinnamic acid (2 mg/ml) in 50% acetonitrile, 0.2% trifluoroacetic acid. A 20-μl aliquot was then spotted onto a hydrophobic H1 protein chip array, and mass identification was performed with a combination of 100 laser shots through each spot with a Ciphergen SELDI Protein Biology System II (PBSII). Sequence assignment of each peak was made by using PAWS software (Rockefeller University) with the default setting at mass accuracy of 1000 parts per million.

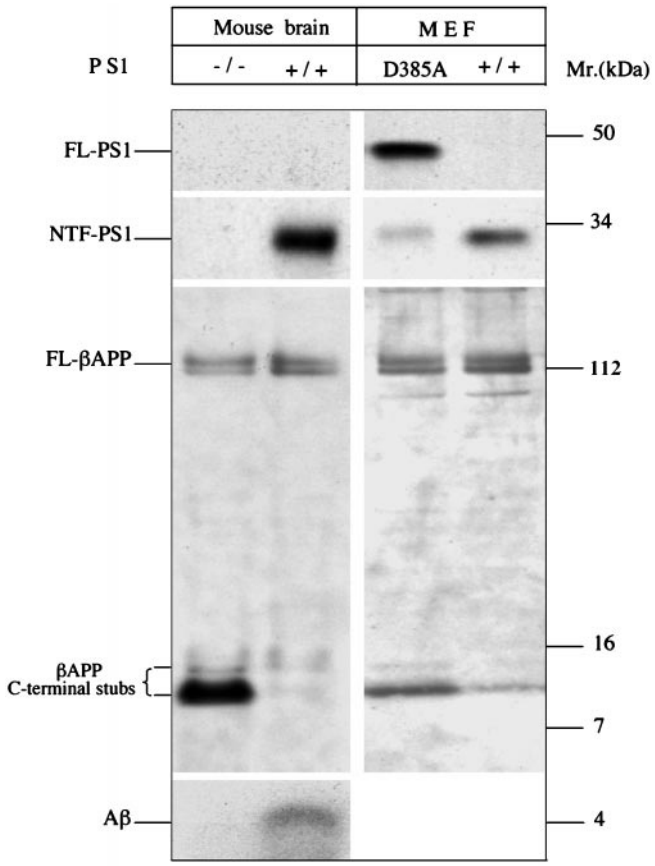

FIG. 2. **Effects of absence of functional PS1 on βAPP processing.** *Upper left*, PS1 Western blots (antibody Ab14) of total lysates from brain homogenates from PS1$^{-/-}$ and PS1$^{+/+}$ mice showing absence of PS1 holoprotein or PS1-NTF in PS1$^{-/-}$ brain. *Middle left*, βAPP Western blot (antibody 369) from the same mouse brain homogenates showing normal amounts and normal glycosylation patterns of *FL-βAPP*, accumulation of βAPP-CTF in the PS1$^{-/-}$ mouse brain homogenates. *Bottom left*, absence of metabolically labeled Aβ in immunoprecipitates from supernatants of neuron cultures from these brains. *Upper right*, PS1 Western blot (antibody Ab14) of whole cell lysates of wild type murine embryonic fibroblasts (*MEF*) and murine embryonic fibroblasts expressing PS1$_{D385A}$ showing accumulation of PS1 holoprotein and suppression of endoproteolysis. *Middle right*, βAPP Western blot (antibody 369) of wild type and PS1$_{D385A}$ fibroblasts showing accumulation of βAPP-CTFs.

RESULTS

Analysis of βAPP processing in brain homogenates from the PS1$^{-/-}$ mice showed normal amounts of *N′*- and *O′*-glycosylated full-length βAPP (Fig. 2). In agreement with previous reports (10–12), there was a dramatic increase in steady state levels of βAPP-CTFs in brain homogenates from PS$^{-/-}$ mice (Fig. 2). A similar increase in steady state levels of CTFs was observed in cells overexpressing the PS1$_{D385A}$ mutation (Fig. 2) (18). Aβ peptide levels were undetectable by enzyme-linked immunosorbent assay in the conditioned media from the PS1$^{-/-}$ and the PS1$_{D385A}$ cells (≤0.02 ng/ml). In contrast, Aβ was easily detectable in the conditioned media of PS1$^{+/+}$ cells (>0.145 ng/ml). The βAPP processing in heterozygous PS1$^{-/+}$ mice was not different from that observed in PS1$^{+/+}$ wild-type mice (data not shown).

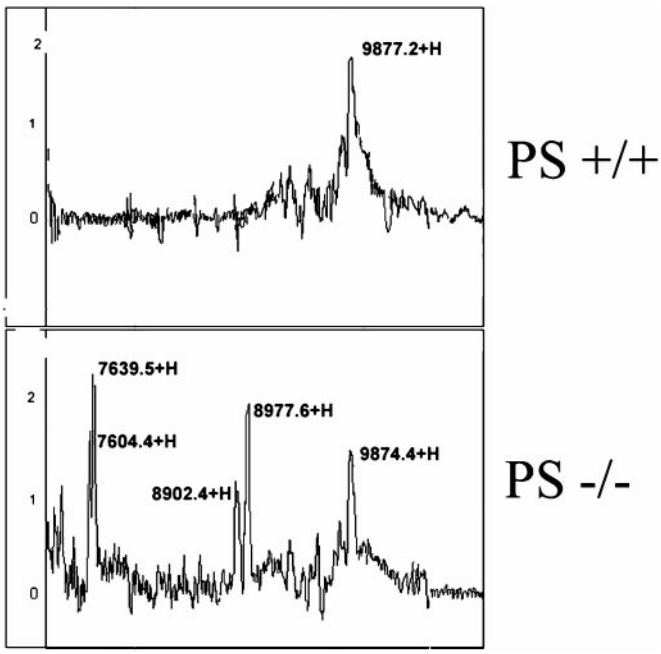

FIG. 3. **Spectra from SELDI analyses of immunoprecipitates of bAPP-CTFs from wild type mice (*upper panel*) and PS1 knock-out mice (*lower panel*).** See Table I for assignment of sequences.

TABLE I
Sequence assignment of major species of βAPP-CTF recovered by immunoprecipitation of PS1$^{-/-}$ mouse brain homogenates (see Fig. 3)

Measured mass	Calculated mass	Predicted sequence
9874.4	9873.5	E[11–98]Q
8977.6	8979.40	D[7–88]N
	8975.40	G[9–90]T
8902.4		Unknown
7639.5	7639.1	R[13–82]Q
7604.9	7604.9	E[3–73]P
	7604.9	F[4–74]E

In order to determine the structure of the βAPP CTFs from the PS1$^{-/-}$ mice, brain homogenates were immunoprecipitated with anti-βAPP COOH-terminal antibodies and mass determined by SELDI-time-of-flight mass spectroscopy using a Ciphergen ProteinChip system. Five major APP CTFs, with mass values of 7604.4, 7639.5, 8902.4, 8977.6, and 9874.4 Da, were detected in the PS$^{-/-}$ brain homogenates (Fig. 3 and Table I). The 9874.4-Da peak represents the major form of βAPP-CTF in the wild type brains (Fig. 3 and Table I) and is identified as βAPP-CTF E[11–98]Q (according to the numbering system of mouse βAPP-C99), which has a calculated mass of 9873.5 Da. This result is consistent with the observation that most Aβ generated by rodent neurons in culture is Aβ-(11–*x*) (Aβ-(11–40), Aβ-(11–42)) (37). No βAPP-CTF-(1–99) or βAPP-CTF-(17–99) were detected.

Species with masses of 7604.9, 7639.5, 8902.4, and 8977.6 Da were specifically associated with PS1 knock-out mice. Computer-assisted sequence assignment indicates that the peak with a mass of 8902.4 Da did not match any known mouse βAPP-CTF and is probably not a βAPP-CTF, but rather a protein recovered due to nonspecific binding of anti-βAPP COOH-terminal antibodies. The 7604.9-Da peak is identical to the calculated mass of E[3–73]P and F[4–74]E. The 7639.5-Da peak is identical to the mass of R[13–82]Q. The 8974.4-Da peak is identical to either D[7–88]N (predicted mass = 8979.40) or G[9–90]T (predicted mass = 8975.40). Determination of βAPP-CTF concentrations based on their relative peak intensities was not meaningful due to the dramatic differences in the binding efficiency between the various CTFs and the matrix.[3]

In order to identify the intracellular sites in which βAPP-CTFs accumulate, we investigated brain and cultured neurons from PS1$^{-/-}$ mice using both morphological and biochemical methods. Particular attention was paid to the ER, Golgi, endosome-lysosome, and caveolae compartments because these organelles have been implicated in Aβ generation. We reasoned that abnormalities in protein trafficking or in γ-secretase catalytic activity in PS1$^{-/-}$ cells would most likely be reflected by changes in the distribution or concentration of CTFs in these compartments. PS1$^{-/-}$ cells were chosen for these analyses instead of the PS1$_{D385A}$ cells because PS1$^{-/-}$ cells can be investigated without potential artifacts arising from overexpression of exogenous mutant PS1$_{D385A}$. No obvious differences were detected in the ultrastructural morphology or number of perinuclear intracytoplasmic membrane bound structures, or in the number or ultrastructural distribution of intracellular membranous structures containing COOH-terminal βAPP immunoreactive epitopes on immunoelectron microscopy (data not shown). However, membranous structures containing CTFs could not be discriminated from those containing FL-βAPP because all available COOH-terminal reactive anti-βAPP antibodies detect both FL-βAPP and its CTFs. Consequently, we also purified membranes from intracellular organelles by biochemical fractionation, which allows FL-βAPP to be distinguished from CTFs on the basis of molecular mass. The purity of these biochemical fractions was verified by ultrastructural morphology (Fig. 1).

Not unexpectedly, lysosomes from PS1$^{-/-}$ brain tissue contained substantial amounts of βAPP-CTFs (Fig. 4). The endocytic pathway has been implicated as a prominent site for Aβ generation (38, 39). However, the amount of βAPP CTFs in late endosome fractions was remarkably low (Fig. 4).

The most intriguing results were obtained from the analysis of gradients containing ER- and Golgi-derived membranes. In the discontinuous sucrose gradients from both PS1$^{-/-}$ mouse brain and PS1$_{D385A}$ cells (Fig. 5), there was a discrete accumulation of stubs in fractions 8–11, with lesser amounts in fractions 14–17. Fractions 14–17 contain morphological and biochemical markers of the Golgi apparatus, while fractions 8–11 contain morphologically non-distinctive vesicles devoid of ribosomes, and have previously been referred to as smooth ER (sER) (26) (Fig. 5). Iodixanol gradient analysis of both PS1$^{-/-}$ brain homogenates and PS1$_{D385A}$ cell lysates confirmed that βAPP-CTFs were broadly present throughout the gradient, but the majority were contained in the ER-associated fractions 7–10 (Fig. 6). A βAPP-CTF species of relatively higher molecular mass was present in both the ER and Golgi fractions, and was the main species in the Golgi fractions (Figs. 5 and 6), a result that is in agreement with previous work suggesting that both β- and γ-secretase cleavage can occur in the ER and Golgi and prior to budding from the TGN (39–42). However, although the sucrose gradient gels do not resolve the βAPP-CTFs as well as the gels run for the iodixanol gradients (the weak band above the very intense βAPP-CTF band in Fig. 6 is likely an artifact due to the overloading of the gel rather than a distinct βAPP-CTF species), both fractionation methods revealed significant amounts of CTFs in the ER fractions (Figs. 5 and 6). This result is surprising, in view of evidence that most secretase cleavages occur during transport to (or at) the cell surface (32, 43). Careful inspection of the distribution of CTFs

[3] F. Chen, D.-S. Yang, S. Petanceska, A. Yang, A. Tandon, G. Yu, R. Rozmahel, J. Ghiso, M. Nishimura, D. M. Zhang, T. Kawarai, G. Levesque, J. Mills, L. Levesque, Y.-Q. Song, E. Rogaeva, D. Westaway, H. Mount, S. Gandy, P. St George-Hyslop, and P. E. Fraser, unpublished observations.

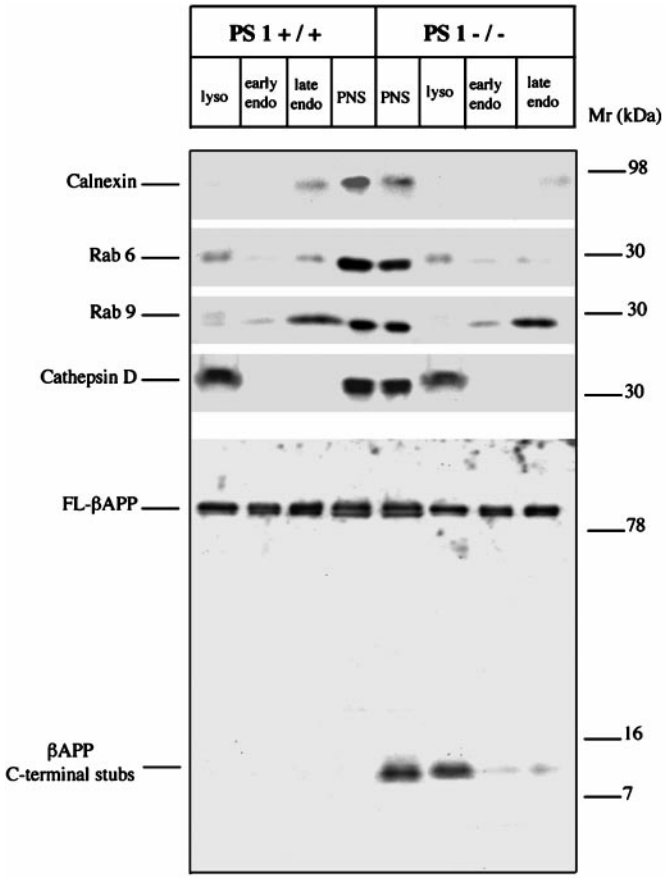

FIG. 4. **Biochemical localization of βAPP holoprotein (FL-βAPP) and CTFs in lysosomal and early and late endosomal fractions of PS1$^{-/-}$ and PS1$^{+/+}$ mouse brain.** Abundant quantities of βAPP-CTFs can be seen in lysosomes (*lyso*) and in the PNS of PS1$^{-/-}$ cells but only very small amounts are present in the early endosomes (*early endo*) and late endosome (*late endo*) compartments. Marker proteins were calnexin (ER), rab 6 (Golgi), rab 9 (endosomes), and cathepsin D (lysosomes).

in the gradients from PS1$_{D385A}$ cell lysates also reveals that, in comparison to PS1$^{-/-}$ cells, the CTFs are less abundant and more restricted to ER fractions, and that only a single major species was consistently apparent, in contrast to the frequently obvious doublet in PS1$^{-/-}$ cells (Figs. 5 and 6). With respect to the apparently distinct patterns of electrophoretic mobility of CTFs from the PS1$^{-/-}$ neurons and the PS1$_{D385A}$ fibroblasts, this is probably due to cell type-specific differences in post-translational modifications such as phosphorylation, since neurons are rich in cdk5 and well documented to phosphorylate the βAPP cytoplasmic domain *in vivo* (44–47). Further, since protein kinases of the cdk family are particularly important in regulating the phosphorylation state of βAPP, the interexperimental differences in the patterns of βAPP CTFs observed when PS1$^{-/-}$ neuronal lysates were analyzed (*e.g.* Fig. 5 *versus* Fig. 6) may well be due to variations in cyclin-dependent protein kinase activities at the various neuronal harvesting times. Mass spectrometry analysis of βAPP-CTFs in the aspartate mutant cells is under way. It is worth noting, however, that these data suggest that there may be subtle differences in the exact mechanisms by which PS1$^{-/-}$ and PS1$_{D385A}$ mutants cause loss of γ-secretase catalytic activity. These differences may be attributable to cell type differences (brain *versus* fibroblasts).

To examine the kinetics of production and intracellular distribution of βAPP-CTFs, we undertook metabolic labeling experiments in cultured PS1$^{+/+}$ and PS1$^{-/-}$ neurons. In agreement with previous work (10), the accumulation of CTFs represented only a minor portion of the total βAPP initially synthesized and occurred after a significant delay (*i.e.* CTFs were undetectable prior to 60 min, and were maximum at 120 min) (data not shown). The generation of βAPP-CTFs in PS1$^{+/+}$ cells appeared to follow a similar time course, although this was difficult to quantify accurately because of the very weak signal intensities for endogenous βAPP-CTFs in PS1$^{+/+}$ neurons (48, 49). Furthermore, the appearance of secreted endogenous βAPP$_s$ in the conditioned medium of PS1$^{-/-}$ cells followed a time course very similar to that in PS1$^{+/+}$ neurons (data not shown). This result contrasts with a previous study, which examined processing of exogenous human βAPP overexpressed in PS1$^{-/-}$ neurons, where the release of βAPP$_{sα}$ occurred abnormally early (11). It is unclear whether this difference reflects an increased sensitivity to small perturbations in βAPP processing that are detectable only in systems overexpressing βAPP, or an artifact of that overexpression system. The fact that the generation of βAPP-CTFs and βAPP$_{sα}$ appears to proceed on schedule in our PS1$^{-/-}$ system using endogenous murine βAPP argues in favor of the latter explanation.

In order to investigate βAPP-CTF metabolism further, we used brefeldin A (BFA), 16 °C temperature block, and NCZ to block forward or retrograde trafficking through the secretory pathway. As expected (50, 51), metabolic pulse-labeling and chase for 4 h in the presence of BFA reduced the maturation of βAPP in both PS1$^{-/-}$ and PS1$^{+/+}$ cultures (Fig. 7). BFA was also found to block the generation of βAPP-CTFs in PS1$^{-/-}$ cells (Fig. 7). This effect was readily reversible. Thus, when BFA was removed from the medium, *N′*- and *O′*-glycosylated βAPP reappeared in PS1$^{-/-}$ and PS1$^{+/+}$ cells, and the βAPP-CTFs reappeared in PS1$^{-/-}$ cells (Fig. 7). These results suggest that βAPP must first traffic to the Golgi compartment before α- or β-cleavage. This interpretation is supported by experiments in which ER-to-Golgi transport was blocked by incubation at 16 °C (Fig. 7), which causes the accumulation of proteins within the ER-Golgi intermediate compartment (52). The maturation of βAPP and the appearance of CTFs were inhibited at 16 °C, but reappeared when the temperature was subsequently shifted to 37 °C (Fig. 7). These results are all consistent with published results using wild-type cells to study βAPP metabolism (53).

NCZ, a microtubule depolymerizing reagent, causes a temporary reduction in forward secretory trafficking and a lasting inhibition of microtubule-dependent retrograde trafficking (*e.g.* from the plasma membrane to endosomes and possibly from Golgi to ER) (54–56). Administration of NCZ to PS1$^{-/-}$ cells did not affect the *O′*-glycosylation of mature βAPP (indicating that βAPP molecules entered the Golgi compartment normally), and did not detectably alter βAPP-CTF levels (Fig. 7). However, NCZ did inhibit the appearance of the higher molecular weight species, but had only a minor effect on the lower molecular weight species (Fig. 7). This suggests that in PS1$^{-/-}$ neurons, a microtubule-dependent retrograde transport event (possibly from the plasma membrane) may be involved in the formation of βAPP-CTFs by regulated proteolysis of βAPP (57).

DISCUSSION

Consistent with other reports (10–12), we have demonstrated that absence of functional PS1, whether generated by null mutations or by missense substitution of conserved aspartate residues, is associated with reduced γ-secretase activity and with accumulation of βAPP-CTFs. However, our data also provide new insights. They suggest that, in the absence of functional PS1, there are subtle changes in the intracellular distribution of βAPP-CTFs, and that in neurons there is accu-

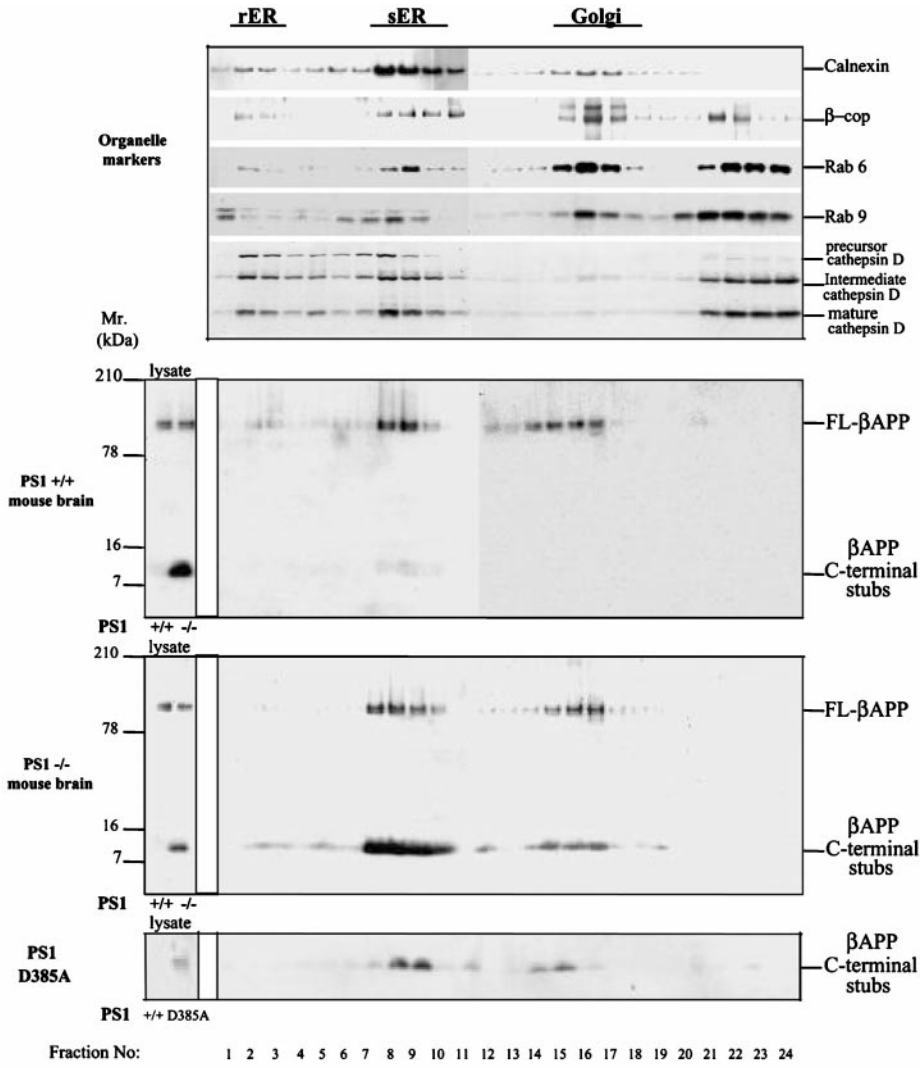

FIG. 5. **Fractionation of rER (*lanes 1–4*), sER (*lanes 8–11*), and Golgi (*lanes 15–17*) from discontinuous sucrose gradients demonstrates discrete accumulation of βAPP-CTFs in sER and Golgi membranes from PS1$^{-/-}$ mouse brain and PS1$_{D385A}$ cells but not PS1$^{+/+}$ mouse brain or normal cells (data not shown).** *Left two lanes* in each panel are total cell lysates from PS1$^{-/-}$, PS1$^{+/+}$ mouse brain, or wild type and PS1$_{D385A}$ cells. The remaining lanes are sequential fractions from bottom (*left*) to top (*right*) of gradient. The distributions of other organelle markers are shown in the *upper panels* (see "Materials and Methods" for marker specificities), and those of species under study (markers and βAPP derivatives) are labeled at the *right* of each panel.

mulation not only of the predominant βAPP-CTF-(11–98) species present in wild type neurons, but also of several other species, that are not simple degradation products of this physiologic βAPP-CTF-(11–98) species.

The elevated βAPP-CTF levels provide enhanced sensitivity for studying the βAPP processing events that generate them. Thus, the accumulation of βAPP-CTFs in the ER and the preponderance of putative β-stubs in the Golgi are consistent with prior data suggesting that the ER-*cis*-Golgi intermediate compartment is one site for the production of Aβ (39–42, 58). Our results are also consistent with the observation that most secretase activity predominantly occurs late in the secretory pathway after βAPP exits the TGN (30, 32, 59, 60). Moreover, our data support the notion that only a minority of βAPP molecules enter a pathway that would lead to γ-secretase cleavage and Aβ production, an observation that again concurs with prior work (61, 62). Finally, our pulse-chase studies reveal that, even when functional PS1 is absent, the CTFs from endogenous βAPP do not accumulate in the first 20–60 min, as might have been predicted if PS1 function or α/β- and γ-secretase cleavage simply represented "quality control" processing events during the initial stages of βAPP biogenesis. Instead, the levels of CTFs are maximal at 80–120 min. This suggests that, in PS1-deficient cells, α/β-secretases act upon βAPP molecules in late compartments. This interpretation is compatible with work suggesting that glycosylation of βAPP in wild type cells occurs prior to α- and β-secretase cleavage (63, 64). The appearance of CTFs in earlier compartments in PS1$^{-/-}$ cells (*e.g.* the ER and Golgi), however, does raise the possibility that CTFs are subsequently transported back to these early compartments (see below).

There are also several unexpected results that would not have been predicted based on published data regarding the intracellular sites of Aβ generation. Although concurring with prior reports on βAPP-CTF distributions in PS1$^{-/-}$ cells (11, 12), the substantial accumulation of CTFs in ER fractions (or an ER-like fraction such as autophagic vacuoles) is surprising. This would not be predicted to occur because previous studies have suggested that both secretase activities occur predominantly after the TGN, at or near the cell surface, and possibly in caveolae (30, 32, 59). One explanation for the presence of CTFs in ER fractions of PS1-deficient cells is that our ER fractions are contaminated with membranes derived from other organelles or the cell membrane. This would be supported by the fact that these fractions do contain small amounts of membranes immunoreactive for markers of other organelles. However, several observations argue this result is not artifactual. First, there was the significant enrichment (>9-fold) of COOH-terminal stubs (as well as calnexin, cathepsin D precursor and *N*′-glycosylated βAPP, which are normally resident only in the ER) in our ER fractions relative to the weaker enrichment (<3-fold) of non-ER/Golgi marker proteins. Second, electron microscopy examination of the sER fractions revealed only smooth vesicles devoid of ribosomes or lysosomes, suggest-

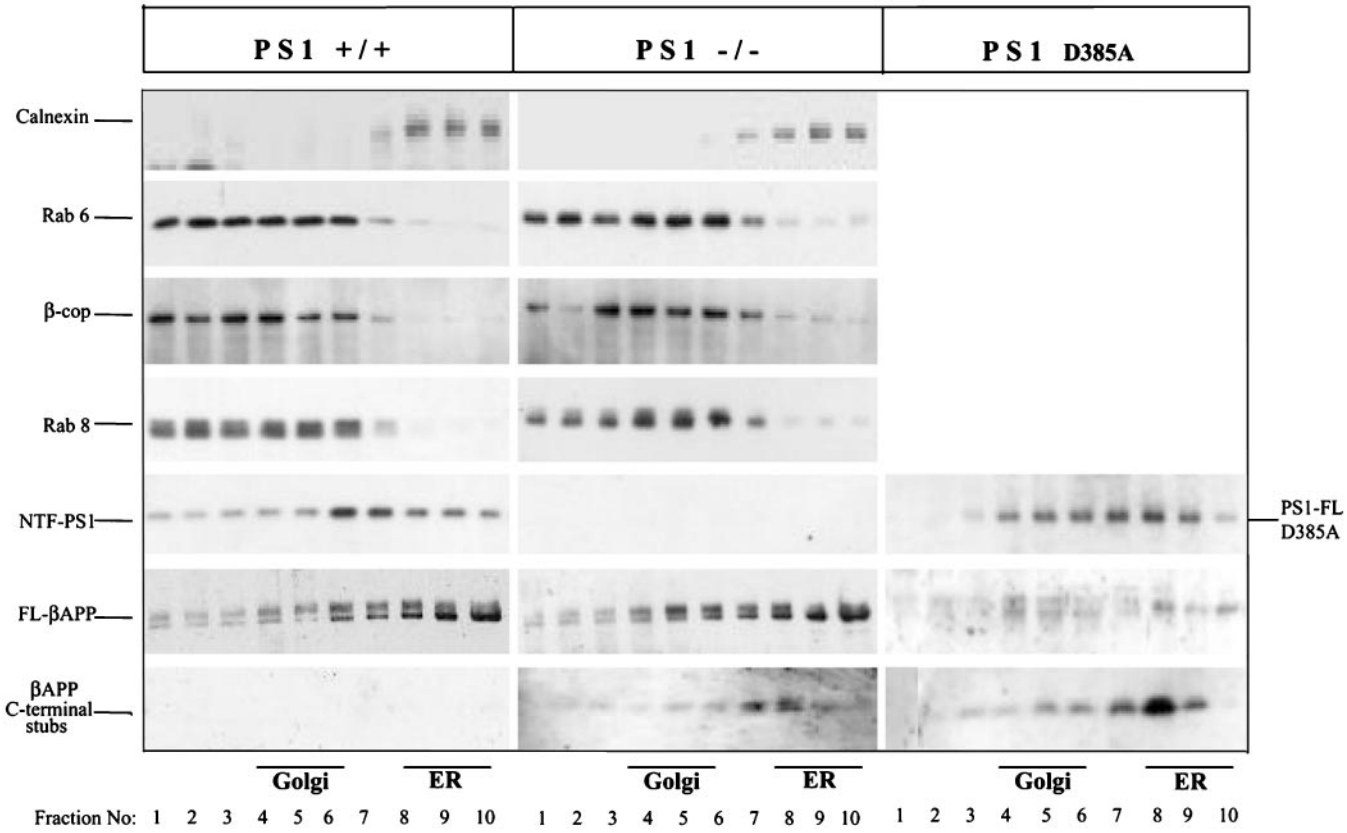

FIG. 6. **Distribution of ER (*lanes 8–10*) and Golgi (*lanes 4–6*) fractions using iodixanol gradients.** Note the subtle difference in speciation of βAPP-CTFs in $PS1^{-/-}$ mouse brain and of $PS1_{D385A}$ fibroblasts.

ing that these fractions contain authentic ER/ER-like membranes, and are not significantly contaminated with non-ER membranes. Consequently, it is likely either that there is some secretase activity in the ER (65), or more probably, that in PS1-deficient cells at least, βAPP-CTFs are retrogradely trafficked to the ER (or an ER-derived compartment such as autophagic vacuoles) from other organelles such as the plasma membrane, TGN, or clathrin-coated vesicles. We have recently used a panel of mutagenesis, subcellular fractionation, immunofluorescence, and metabolic labeling approaches to provide strong evidence that PS1 can control γ-secretase processing of βAPP stubs in pre-Golgi compartments of hippocampal neurons (66). These published results support our conclusion that, in $PS1^{-/-}$ and $PS1_{D385A}$ cells, some βAPP-CTFs may be targeted to a pre-Golgi, ER-like compartment. Finally, it is worth noting that we were able to discern subtle differences between the distribution and apparent electrophoretic speciation of βAPP-CTFs in the $PS1^{-/-}$ mouse brain compared with that in $PS1_{D385A}$ mutant fibroblasts. This disparity may be attributable to cell type differences (*i.e.* brain *versus* fibroblasts). However, it clearly raises the possibility that there are subtle differences in the exact mechanisms by which aspartate mutants cause loss of γ-secretase activity.

The accumulation of βAPP-CTFs in lysosomes but not in late endosomes can be interpreted in several ways. First, it is quite possible that the lysosomal fractions prepared by us and by others contain some contamination by the βAPP-CTF-rich, sER-like fractions that we have identified. In this regard, it is worth noting that fractions containing the highest enrichment for the mature low molecular weight isoform of the lysosomal marker cathepsin D (Fig. 5, fractions 20–24) are devoid of detectable βAPP-CTF immunoreactivity. Second, it is conceivable that the accumulation of βAPP-CTFs in lysosomes of PS1-deficient cells may simply reflect a trivial result, namely non-specific targeting of unprocessed CTFs into this compartment for terminal degradation. Third, prior work has suggested that $A\beta_{40}$ may be generated in the lysosome-late endosome compartments from βAPP returning from the cell surface (38, 67), and βAPP-CTFs have been observed in lysosomes and clathrin-coated vesicles (30, 68). These data suggest that, in wild-type cells, COOH-terminal stubs are normally targeted for degradation in the endocytic pathway. Our data showing βAPP-CTFs in lysosomes would appear to confirm the latter observations. Finally, it is also possible that the massive accumulation of CTFs in lysosomes and their paucity in the endosome precursors in PS1-deficient cells represent a specific disturbance of normal βAPP processing in the endocytic pathway in the absence of PS1. Indeed, we cannot exclude the possibility that, in $PS1^{-/-}$ cells, βAPP-CTFs bypass the endosomal system and traffic directly to lysosomes. Such a scenario could plausibly underlie the failure of $PS1^{-/-}$ cells to generate Aβ.

Mass spectrometry analysis of immunoprecipitated βAPP-CTFs has also demonstrated significant differences in their processing based on the appearance of $PS^{-/-}$ specific species. In wild-type neurons, the predominant CTF corresponded to the 11–98 sequence, suggesting that, under normal conditions, subsequent γ-secretase cleavage would lead to production of Aβ peptides containing residues 11–40/42, as has previously been reported (37). This finding has implications for the potential contribution of such Aβ species to the generation of senile plaques as it has, for example, been demonstrated *in vitro* that these truncated peptides are actually more amyloidogenic than the full-length Aβ protein (69–71). In the case of $PS1^{-/-}$ neurons, we observed several additional unique βAPP-CTFs that, based on their NH_2- and COOH-terminal heterogeneity (*e.g.* 4–74 and 7–90), do not appear to arise through processing of the wild-type 11–98 fragment. The amino-terminal data are potentially consistent with the observation that amyloid

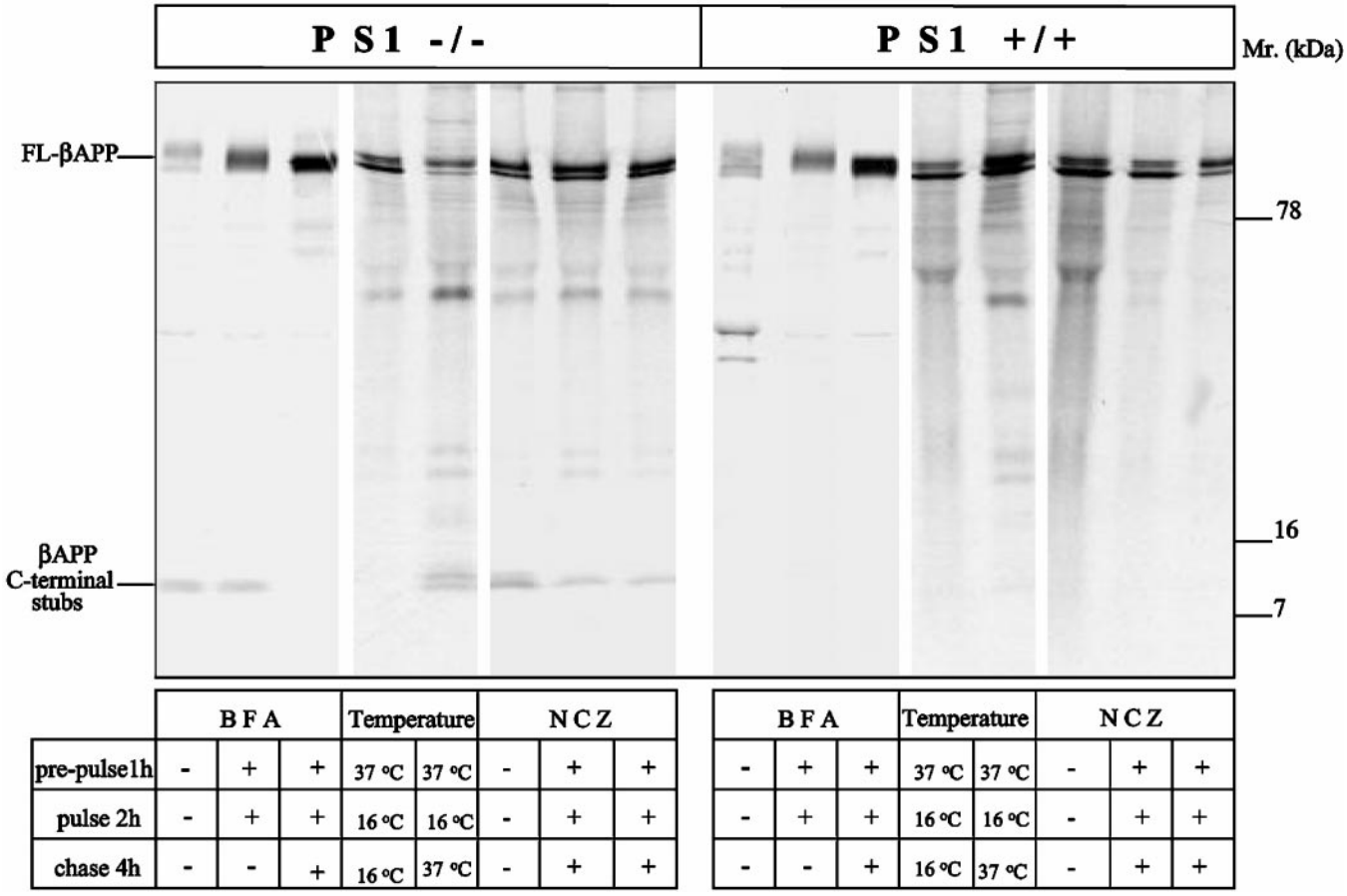

FIG. 7. **Metabolic labeling and immunoprecipitation studies of FL-βAPP and βAPP CTFs show that the formation of endogenous βAPP-CTFs is prevented by incubation at 16 °C or in BFA, both of which block ER → Golgi trafficking.** Formation of CTFs is restored by reversion to 37 °C or by washing out BFA. Formation of the higher mass, putative β-CTFs is significantly impaired following blockade of retrograde trafficking by NCZ, while the putative α-CTFs are affected to a lesser extent (*lanes 7* and *8* and *lanes 15* and *16* are replica experiments; note that nocodozaole cannot be efficiently removed from cells in the chase period).

plaques contain Aβ species beginning at Aβ3, Aβ4, Aβ6, Aβ7, Aβ8, Aβ9, and Aβ11 (72). In the PS1$^{-/-}$ mice, the massive accumulation of CTFs may lead to the accumulation of these presumably quantitatively minor species. However, these novel fragments could also be generated via alternate processing pathways resulting from the loss of functional PS1, or they could indicate a more generalized disruption of the normal proteolysis of the fragments generated by the α- and β-secretases.

The alterations in the distribution of βAPP-CTFs in PS1-deficient cells are relatively subtle. These changes do not strongly support a model for PS1 function which involves control of major, fundamental aspects of general protein trafficking (*e.g.* of the organelle marker proteins used in these studies) or of FL-βAPP in particular. In support of this, we have shown previously that absence of PS1 does not significantly affect trafficking of β-catenin, a known PS1 ligand (however, pathogenic gain-of-function mutations do affect β-catenin trafficking to the nucleus (see Ref. 8)). We cannot exclude a more restricted role for PS1 in trafficking of βAPP-CTFs, but the subtle nature of the observed alterations in CTF distribution in PS1-deficient cells would not seem sufficient to account for the profound alteration in γ-secretase activity. Our data therefore are most consistent with the interpretation that PS1 either is the γ-secretase active site (or is a component of a γ-secretase complex, for example, as a γ-secretase activating cofactor or a βAPP-γ-secretase adaptor protein), or is closely, but indirectly, involved in γ-secretase proteolysis (*e.g.* as a modulator of delivery of γ-secretase to α- and β-stub-containing compartments). Our documentation that the major accumulating βAPP-CTF is probably βAPP-CTF-(11–98) underscores the importance of the utilization of the cleavage of Aβ between residues 10 and 11 by β-secretase (73). This result may have implications for the potential toxicity of therapeutic γ-secretase inhibitors since Aβ-(11–98) may itself aggregate (74) and/or undergo nonspecific proteolysis and release amyloidogenic peptides (75). These results also raise the possibility that Aβ-(11–40) and Aβ-(11–42) peptides are important in the pathobiology of Aβ aggregation, deposition, clearance, and toxicity associated with Alzheimer's disease. Finally, these data underscore the importance of mass and/or sequence analysis for the accurate assignment of identities to βAPP-CTFs.

Acknowledgments—We thank Dr. E. Koo and F. Checler for the kind gifts of antibodies 5A3/1G7 and FCA18, respectively.

REFERENCES

1. Sherrington, R., Rogaev, E., Liang, Y., Rogaeva, E., Levesque, G., Ikeda, M., Chi, H., Lin, C., Holman, K., Tsuda, T., Mar, L., Fraser, P., Rommens, J. M., and St. George-Hyslop, P. (1995) *Nature* **375,** 754–760
2. Rogaev, E. I., Sherrington, R., Rogaeva, E. A., Levesque, G., Ikeda, M., Liang, Y., Chi, H., Lin, C., Holman, K., Tsuda, T., Mar, L., Sorbi, S., Nacmias, B., Piacentini, S., Amaducci, L., Chumakov, I., Cohen, D., Lannfelt, L., Fraser, P. E., Rommens, J. M., and St. George-Hyslop, P. (1995) *Nature* **376,** 775–778
3. Capell, A., Grunberg, J., Pesold, B., Diehlmann, A., Citron, M., Nixon, R., Beyreuther, K., Selkoe, D. J., and Haass, C. (1998) *J. Biol. Chem.* **273,** 3205–3211
4. Yu, G., Chen, F., Levesque, G., Nishimura, M., Zhang, D.-M., Levesque, L., Rogaeva, E., Xu, D., Liang, Y., Duthie, M., St. George-Hyslop, P., and Fraser, P. E. (1998) *J. Biol. Chem.* **273,** 16470–16475
5. Walter, J., Capell, A., Grunberg, J., Pesold, B., Schindzielorz, A., Prior, R.,

Podlisny, M. B., Fraser, P., St. George-Hyslop, P., Selkoe, D., and Haass, C. (1996) *Mol. Med.* **2,** 673–691
6. De Strooper, B., Beullens, M., Contreras, B., Craessaerts, K., Moechars, D., Bollen, M., Fraser, P., St. George-Hyslop, P., and Van Leuven, F. (1997) *J. Biol. Chem.* **272,** 3590–3598
7. Levesque, L., Annaert, W., Craessaerts, K., Mathews, P. M., Seeger, M., Nixon, R., van Leuven, F., Gandy, S., Westaway, D., St. George-Hyslop, P., De Strooper, B., and Fraser, P. E. (1999) *Mol. Med.* **5,** 542–554
8. Nishimura, M., Yu, G., Levesque, G., Zhang, D. M., Ruel, L., Chen, F., Milman, P., Holmes, E., Liang, Y., Kawarai, T., Jo, E., Supala, A., Rogaeva, E., Xu, D. M., Janus, C., Levesque, L., Bi, Q., Duthie, M., Rozmahel, R., Mattila, K., Lannfelt, L., Westaway, D., Mount, H. T., Woodgett, J., Fraser, P., and St. George-Hyslop, P. (1999) *Nat. Med.* **5,** 164–169
9. Levesque, G., Yu, G., Nishimura, M., Zhiang, D. M., Levesque, L., Yu, H., Xu, D., Liang, Y., Ikeda, M., Rommens, J., Fraser, P. E., and St. George-Hyslop, P. (1999) *J. Neurochem.* **72,** 999–1008
10. De Strooper, B., Saftig, P., Craessaerts, K., Vanderstichele, H., Guhde, G., Annaert, W., Von Figura, K., and Van Leuven, F. (1998) *Nature* **391,** 387–390
11. Naruse, S., Thinakaran, G., Luo, J. J., Kusiak, J. W., Tomita, T., Iwatsubo, T., Qian, X., Ginty, D. D., Price, D. L., Borchelt, D. R., Wong, P. C., and Sisodia, S. S. (1998) *Neuron* **21,** 1213–1221
12. Xia, W., Zhang, H., Ostaszewski, B. L., Kimberly, W. T., Seubert, P., Koo, E. H., Shen, J., and Selkoe, D. J. (1998) *Biochemistry* **24,** 16465–16471
13. Ye, Y., Lukinova, N., and Fortini, M. E. (1999) *Nature* **398,** 525–529
14. Struhl, G., and Greenwald, I. (1999) *Nature* **398,** 522–525
15. De Strooper, B., Annert, W., Cupers, P., Saftig, P., Craessaerts, K., Mumm, J. S., Schroeter, E. H., Schrijvers, V., Wolfe, M. S., Ray, W. J., Goate, A., and Kopan, R. (1999) *Nature* **398,** 518–522
16. Li, Y. M., Xu, M., Lai, M. T., Huang, Q., Castro, J. L., DiMuzio-Mower, J., Harrison, T., Lellis, C., Nadin, A., Neduvelil, J. G., Register, R. B., Sardana, M. K., Shearman, M. S., Smith, A. L., Shi, X. P., Yin, K. C., Shafer, J. A., and Gardell, S. J. (2000) *Nature* **405,** 689–694
17. Esler, W. P., Kimberly, W. T., Ostaszewski, B. L., Diehl, T. S., Moore, C. L., Tsai, J. Y., Rahmati, T., Xia, W., Selkoe, D. J., and Wolfe, M. S. (2000) *Nat Cell Biol.* **2,** 428–434
18. Wolfe, M. S., Xia, W., Ostaszewski, B. L., Diehl, T. S., Kimberly, W. T., and Selkoe, D. S. (1999) *Nature* **398,** 513–517
19. Yu, G., Chen, F., Nishimura, M., Steiner, H., Tandon, A., Kawarai, T., Arawaka, S., Supala, A., Song, Y.-Q., Rogaeva, E., Holmes, E., Zhang, D.-M., Milman, P., Fraser, P., Haass, C., and St. George-Hyslop, P. (2000) *J. Biol. Chem.* **275,** 27348–27353
20. Shen, J., Bronson, R. T., Chen, D. F., Xia, W., Selkoe, D. S., and Tonegawa, S. (1997) *Cell* **89,** 629–639
21. Wong, P. C., Zheng, H., Chen, H., Becher, M. W., Sirinathsinghji, D. J., Trumbauer, M. E., Chen, H. Y., Price, D. L., Van Der Ploeg, L. H., and Sisodia, S. S. (1997) *Nature* **387,** 288–292
22. Thinakaran, G., Borchelt, D. R., Lee, M. K., Slunt, H. H., Spitzer, L., Kim, G., Ratovisky, T., Davenport, F., Nordstedt, C., Seeger, M., Levey, A. I., Gandy, S. E., Jenkins, N. A., Copeland, N., Price, D. L., and Sisodia, S. S. (1996) *Neuron* **17,** 181–190
23. Watt, C. B., Su, Y. Y. T., and Lam, D. M. K. (1985) *J. Neurosci.* **5,** 875–865
24. Tjelle, T. E., Brech, A., Juvet, L. K., Griffiths, G., and Berg, T. (1996) *J. Cell Sci.* **109,** 2905–2914
25. Lupashin, V. V., Hamamoto, S., and Schekman, R. W. (1996) *J. Cell Biol.* **132,** 277–289
26. Bole, D. G., Hendershot, L. M., and Kearney, J. F. (1986) *J. Cell Biol.* **102,** 1558–1566
27. Lukacs, G. L., Mohamed, A., Kartner, N., Chang, X.-B., Riordan, J. R., and Grinstein, S. (1994) *EMBO J.* **13,** 6076–6086
28. Majoul, I. V., Bastiaens, P. I. H., and Soling, H. D. (1996) *J. Cell Biol.* **133,** 777–789
29. Gorvel, J.-P., Chavier, P., Zerial, M., and Gruenberg, J. (1991) *Cell* **64,** 915–925
30. Haass, C., Koo, E. H., Mellon, A., Hung, A. Y., and Selkoe, D. J. (1992) *Nature* **357,** 500–503
31. Lee, S.-J., Liyanage, U., Bickel, P., Xia, W., Lansbury, P. T., and Kosik, K. (1998) *Nat. Med.* **4,** 730–734
32. Ikezu, T., Trapp, B. D., Song, K. S., Schlegel, A., Lisanti, M. P., and Okamoto, T. (1998) *J. Biol. Chem.* **273,** 10485–10495
33. Bickel, P. E., Scherer, P. E., Schnitzer, J. E., Oh, P., Lisanti, M. P., and Lodish, H. F. (1997) *J. Biol. Chem.* **272,** 13793–13802
34. Parkin, E. T., Hussain, I., Turner, A. J., and Hooper, N. M. (1997) *J. Neurochem.* **69,** 2179–2188
35. Stan, R.-V., Roberts, W. G., Predescu, D., Ihida, K., Saucan, L., Ghitescu, L., and Palade, G. E. (1997) *Mol. Biol. Cell* **8,** 595–605
36. Barelli, H., Lebeau, A., Vizzavona, J., Delaere, P., Chevallier, N., Drouot, C., Marambaud, P., Ancolio, K., Buxbaum, J. D., Martinez, J., Warter, J.-M., Mohr, M., and Checler, F. (1997) *Mol. Med.* **3,** 695–707
37. Gouras, G. K., Xu, H., Jovanovic, J. N., Buxbaum, J. D., Wang, R., Greengard, P., Relkin, N. R., and Gandy, S. (1998) *J. Neurochem.* **71,** 1920–1925
38. Koo, E. H., and Squazzo, S. L. (1994) *J. Biol. Chem.* **269,** 17386–17389
39. Hartmann, T., Beiger, S., Bruhl, B., Tienari, P. J., Ida, N., Roberts, G., Allsop, D., Masters, C. L., Dotti, C. G., Unsicker, K., and Beyreuther, K. (1997) *Nat. Med.* **3,** 1016–1020
40. Cook, D. G., Forman, M., Sung, J. C., Leight, S., Kolson, D. L., Iwatsubo, Y., Lee, V. M.-Y., and Doms, R. W. (1997) *Nat. Med.* **3,** 1021–1023
41. Wild-Bode, C., Capell, A., Yamazaki, T., Leimer, U., Steiner, H., Ihara, Y., and Haass, C. (1997) *J. Biol. Chem.* **272,** 16085–16088
42. Xu, H., Sweeney, D., Wang, R., Thinakaran, G., Lo, A. C. Y., Sisodia, S. S., Greengard, P., and Gandy, S. (1997) *Proc. Natl. Acad. Sci. U. S. A.* **94,** 3748–3752
43. Sisodia, S. S., Koo, E. H., Beyreuther, K., Unterbeck, A., and Price, D. (1990) *Science* **248,** 492–495
44. Suzuki, T., Oishi, M., Marshak, D. R., Czernik, A. J., Nairn, A. C., and Greengard, P. (1994) *EMBO J.* **13,** 1114–1122
45. Oishi, M., Nairn, A. C., Czernik, A. J., Lim, G. S., Isohara, T., Gandy, S. E., Greengard, P., and Suzuki, T. (1997) *Mol. Med.* **3,** 111–123
46. Buxbaum, J. D., Thinakaran, G., Koliatsos, V., O'Callahan, J., Slunt, H. H., Price, D. L., and Sisodia, S. S. (1998) *J. Neurosci.* **18,** 9629–9637
47. Iijima, K., Ando, K., Takeda, S., Satoh, Y., Seki, T., Itohara, S., Greengard, P., Kirino, Y., Nairn, A. C., and Suzuki, T. (2000) *J. Neurochem.* **75,** 1085–1091
48. Refolo, L. M., Sambamurti, K., Efthimopoulos, S., Pappolla, M. A., and Robakis, N. K. (1995) *J. Neurosci. Res.* **40,** 694–706
49. Sambamurti, K., Shioi, J., Anderson, J. P., Pappolla, M. A., and Robakis, N. K. (1992) *J. Neurosci. Res.* **33,** 319–329
50. Sciaky, N., Presley, J., Smith, C., Zaal, K. J., Cole, N., Moriera, J. E., Terasaki, M., Siggia, E., and Lippincott-Schwartz, J. (1997) *J. Cell Biol.* **139,** 1137–1155
51. Caporaso, G. L., Gandy, S. E., Buxbaum, J. D., Ramabhadran, T. V., Greengard, P. (1992) *Proc. Natl. Acad. Sci. U. S. A.* **89,** 3055–3059
52. Saraste, J., and Kuismanen, E. (1984) *Cell* **38,** 535–549
53. Caporaso, G. L., Gandy, S. E., Buxbaum, J. D., and Greengard, P. (1992) *Proc. Natl. Acad. Sci. U. S. A.* **89,** 2252–2256
54. Storrie, B., and Yang, W. (1998) *Biochim. Biophys. Acta* **1404,** 127–137
55. Thyberg, J., and Moskalewski, S. (1999) *Exp. Cell Res.* **246,** 263–279
56. Jin, M., and Snider, M. D. (1993) *J. Biol. Chem.* **268,** 18390–13897
57. Perez, R. G., Soriano, S., Hayes, J. D., Ostaszewski, B., Xia, W., Selkoe, D. J., Chen, X., Stokin, G. B., and Koo, E. H. (1999) *J. Biol. Chem.* **274,** 18851–18856
58. Greenfield, J. P., Tsai, J., Gouras, G. K., Hai, B., Thinakaran, G., Checler, F., Sisodia, S. S., Greengard, P., and Xu, H. (1999) *Proc. Natl. Acad. Sci. U. S. A.* **96,** 742–747
59. Sisodia, S. (1993) *Proc. Natl. Acad. Sci. U. S. A.* **89,** 6075–6079
60. Petanceska, S., Seeger, M., Checler, F., and Gandy, S. (2000) *J. Neurochem.* **74,** 1878–1884
61. Haass, C., Schlossmacher, M. G., Hung, A. Y., Vigo-Pelfrey, C., Mellon, A., Ostaszewski, B. L., Lieberburg, I., Koo, E. H., Schenk, D., Teplow, D. B., and Selkoe, D. J. (1992) *Nature* **359,** 322–325
62. Seubert, P., Vigo-Pelfrey, C., Esch, F., Lee, M., Dovey, H., Davis, D., Selkoe, D., Lieberburg, I., and Schenk, D. (1992) *Nature* **359,** 325–327
63. Caporaso, G. L., Takei, K., Gandy, S. E., Matteoli, M., Mundigl, O., Greengard, P., and De Camilli, P. (1994) *J. Neurosci.* **14,** 3122–3138
64. Tomita, S., Yukata, K., and Suzuki, T. (1998) *J. Biol. Chem.* **273,** 6277–6284
65. Lammich, S., Kojro, E., Postina, R., Gilbert, S., Pfeiffer, R., Jasionowski, M., Haass, C., and Fahrenholz, F. (1999) *Proc. Natl. Acad. Sci. U. S. A.* **96,** 3922–3927
66. Annaert, W. G., Levesque, L., Craessaerts, K., Dierinck, I., Schellings, D., Westaway, D., St. George-Hyslop, P., Cordell, B., Fraser, P., and De Strooper, B. (1999) *J. Cell Biol.* **147,** 277–294
67. Peraus, G. C., Masters, C. L., and Beyreuther, K. (1997) *J. Neurosci.* **15,** 7714–7724
68. Nordstedt, C., Caporaso, G. L., Thyberg, J., Gandy, S. E., and Greengard, P. (1993) *J. Biol. Chem.* **268,** 608–612
69. Hilbich, C., Kisters-Woike, B., Reed, J., Masters, C. L., and Beyreuther, K. (1991) *J. Mol. Biol.* **218,** 149–163
70. Hilbich, C., Kisters-Woike, B., Reed, J., Masters, C. L., and Beyreuther, K. (1992) *J. Mol. Biol.* **228,** 460–473
71. Pike, C. J., Overman, M. J., and Cotman, C. W. (1995) *J. Biol. Chem.* **270,** 23895–23898
72. Naslund, J., Schierhorn, A., Hellman, U., Lannfelt, L., Roses, A. D., Tjernberg, L. O., Silberring, J., Gandy, S. E., Winblad, B., Greengard, P., Nordstedt, C., and Terenius, L. (1994) *Proc. Natl. Acad. Sci. U. S. A.* **91,** 8378–8382
73. Vassar, R., Bennett, B. D., Babu-Kahn, S., Kahn, S., Mendiaz, E. A., Denis, P., Teplow, D. W., Ross, S., Amarante, P., Loeloff, R., Luo, Y., Fisher, S., Fuller, J., Fuller, J., Louis, J. C., Collins, F., Treanor, J., Rogers, G., and Citron, M. (1999) *Science* **286,** 735–741
74. Gardella, J. E., Gorgone, G. A., Candela, L., Ghiso, J., Castano, E. M., Frangione, B., and Gorevic, P. D. (1993) *Biochem. J.* **294,** 667–674
75. Tjernberg, L. O., Naslund, J., Thyberg, J., Gandy, S. E., Terenius, L., and Nordstedt, C. (1997) *J. Biol. Chem.* **272,** 1870–1875